HAL open science

Evidence for coupled seismic and aseismic fault slip during water injection in the geothermal site of Soultz (France), and implications for seismogenic transients

Seid Bourouis, Pascal Bernard

To cite this version:

Seid Bourouis, Pascal Bernard. Evidence for coupled seismic and aseismic fault slip during water injection in the geothermal site of Soultz (France), and implications for seismogenic transients. Geophysical Journal International, 2007, 169 (2), pp.723-732. 10.1111/j.1365-246X.2006.03325.x . hal-00310546

HAL Id: hal-00310546

https://hal.science/hal-00310546

Submitted on 16 Jun 2017

HAL is a multi-disciplinary open access archive for the deposit and dissemination of scientific research documents, whether they are published or not. The documents may come from teaching and research institutions in France or abroad, or from public or private research centers.

L'archive ouverte pluridisciplinaire **HAL**, est destinée au dépôt et à la diffusion de documents scientifiques de niveau recherche, publiés ou non, émanant des établissements d'enseignement et de recherche français ou étrangers, des laboratoires publics ou privés.

Geophys. J. Int. (2007) **169,** 723–732 doi: 10.1111/j.1365-246X.2006.03325.x

Evidence for coupled seismic and aseismic fault slip during water injection in the geothermal site of Soultz (France), and implications for seismogenic transients

Seid Bourouis[1,2] and Pascal Bernard[1]

[1]*Institut de Physique, du Globe de Paris,* 4 *Place Jussieu* 75252*, Paris Cedex* 05*, France. E-mail: bernard@ipgp.jussieu.fr*
[2]*CRAAG, Algeria*

Accepted 2006 December 7. Received 2006 December 7; in original form 2006 February 9

SUMMARY

We analysed the triggered seismicity recorded near 3 km in depth within granite during the 1993 water injection experiment at Soultz (France). We selected all large multiplets associated with the largest dislocated fault identified on the borehole logging (4.3 cm slip), and showed that each one consisted of the repeated rupture of a single asperity. These asperities were forced to rupture due to fault creep around them, so that their growing, cumulative slip history reveals the creep history on the fault, with a mean slip rate and a seismicity rate both decaying approximately as $1/t$. This is consistent with a rate-strengthening friction law on the creeping faults, and differs from the interpretation of Omori type $1/t$ seismicity rates in terms of a weakening friction control of the unstable fault surfaces. This model of asperity rupture forced by relaxation creep is easily generalized in seismogenic regions, even for single ruptures of asperities on small creeping faults, showing that a significant part of aftershock rates can be controlled by the strengthening friction properties and the creep of faults at all scales. This lead us to introduce the concept of a critical asperity density, above which dynamic interaction between neighbouring asperities can initiate large seismic ruptures. At Soultz, the asperity density is subcritical, but the neighbouring asperities nonetheless interact, at distances up to a few source dimensions, as revealed by their delayed cross-triggering. Considering the seismic cloud in Soultz at a global scale, the strain produced by the injection experiment was mostly aseismic, related to creep on major faults, and causing large permeability changes – influencing in turn the pore pressure diffusion and the creeping process. Our observations demonstrate that the identification and analysis of multiplets can provide accurate images of the geometry and kinematics of transient slip patches, and indirectly detect pore pressure changes, which should contribute to a better understanding of the coupling between transient fluid flow, creep and microseismic activity in seismogenic regions.

Key words: aftershocks, crustal deformation, fluids in rocks, seismicity.

1 INTRODUCTION

In seismogenic regions, strain transient processes have been observed for decades. They can last minutes to years, and are associated to fault creep, seismic swarm activity, and/or fluid flow instabilities. Seismic swarms are the most common transients in a seismogenic crust. These clusters of small to moderate earthquakes can be interpreted with three different, speculative end-models: (1) a direct mechanical interaction between events through their static (Stein 1999) and/or dynamic (Gomberg *et al.* 2001) stress field; (2) triggering caused by silent creep on a large fault segment (e.g. Linde *et al.* 1996) and (3) a natural hydrofracturation or hydrostimulation process, (e.g. Bosl & Nur 2002; Hainzl & Fisher 2002).

The usual absence of direct measurement of fluid flow or creep within fault zones at depth, during seismic swarm activity, has favoured the first approach, that is, the interpretation of the seismic clustering in terms of earthquake cross-triggering (e.g. Helmstetter & Sornette 2003). This approach would clearly be very misleading in case of a fluid or creep transient source process. Unfortunately, the latter are extremely difficult to detect and constrain. Fluid instabilities in the deep crust are only inferred from the evidence of multiphasing cementation of veins and fractures (e.g. Hickman *et al.* 1995), possibly related with earthquake triggering (Sibson 1992). Episodic fault creep is better documented, in the shallowest part of the crust (e.g. Gladwin *et al.* 1994; Gwyther *et al.* 1996), and now inferred at greater depths for the post-seismic phase (e.g. Bürgmann *et al.* 2002). For the latter, afterslip is modelled by rate-strengthening friction laws (Dieterich 1978; Scholz 1998). For the creep transients recently discovered in subduction zones (Dragert *et al.* 2001; Lowry *et al.* 2001; Miller *et al.* 2002; Shibazaki & Iio 2003), water is

© 2007 The Authors
Journal compilation © 2007 RAS

supposed to play an important role, but the leading mechanics remains unclear.

Thus, there is presently a large variety of plausible, although poorly constrained physical models of seismic, creep and pore pressure transients, and of their coupling processes. In this context, the Soulz-sous-Forêt (Alsace, France) 1993 hot dry rock geothermal experiment, with the injection of 25 000 m^3 of water within granite around 3 km in depth, has provided a rare opportunity to precisely measure and analyse such processes. Indeed, the controlled water pressure stimulation at Soultz triggered a well recorded, strong microseismic activity, as well as major fracture slip revealed by the post-experiment borehole loggings.

In this paper, we fist present our analysis and mechanical interpretation of the fluid–creep–seismic coupled process from a selected set of the Soultz seismic records. We then discuss the implication of the proposed model in the context of transients within natural seismogenic regions.

2 THE 1993 WATER INJECTION EXPERIMENT

The geothermal field of Soultz-sous-Forêt is located in the Rhine graben (Alsace, France), within the granitic rock basement, covered by 1.4 km of Mesozoic sediments (Elsass *et al.* 1995). The first large-scale experiment at Soultz, in 1993, involved the injection of 25 000 m^3 of water in a deep borehole, opened from 2.9 to 3.5 km. The injection lasted 17 d, with increasing pressure reaching 10 MPa. It generated a large swarm of microearthquakes, in the magnitude range −0.5 to 1.9 (Heim 1996), starting from the top of the injection column, and growing with an ellipsoidal shape with time for eventually reaching 2 km vertically, 1.5 km in the NNW direction, and 0.6 km in the ENE direction (Jones *et al.* 1995). This seismic activity was accompanied by an important enhancement of permeability (Evans *et al.* 2005), and the migration of seismicity could be related with pore pressure diffusion (Shapiro *et al.* 1999; Cornet 2000) (Fig. 1). More than 12 000 events were located thanks to a downhole array of 3 three-component seismometers and one hydrophone (5 KHz sampling rate), at 1.4–2 km in depth, above the seismic cloud. The absolute location uncertainty is 30, 60 and 20 m in the E, N and vertical directions, respectively.

Borehole logging before and after the injection revealed that a few fractures with high dip angle slipped during the injection phase, with slip values ranging from a few millimetres up to more than 4 cm (Cornet *et al.* 1997). Although the latter value corresponds to the typical slip of a magnitude 3.5 earthquake, with fault length of several hundreds of metres, the largest reported magnitude for the swarm is 1.9, implying that these large dislocations occurred by creep on a few faults, which is the focus of the present paper.

3 MULTIPLET SELECTION AND ANALYSIS: REPEATED RUPTURE OF SINGLE ASPERITIES

Following the preliminary work by Gaucher (1998), we conducted a systematic search for multiplets (i.e. repeating seismic waveforms, diagnostic of the rupture of neighbouring faults with similar mechanism) on the whole data base of seismograms (Bourouis 2004). We found that more than half of the earthquakes could be grouped as doublets or as larger multiplets with waveform correlation larger than 0.9 (Fig. 2a). More than 130 multiplets consisted of more than five earthquakes each, representing a total of about 1500 events. The largest one had 54 events. The accurate relocation of these events allowed to identify fine structures, undetectable by the 'collapsing method' used by Evans *et al.* (2005), and to propose a new hydromechanical model for the Soultz experiment (Bourouis 2004).

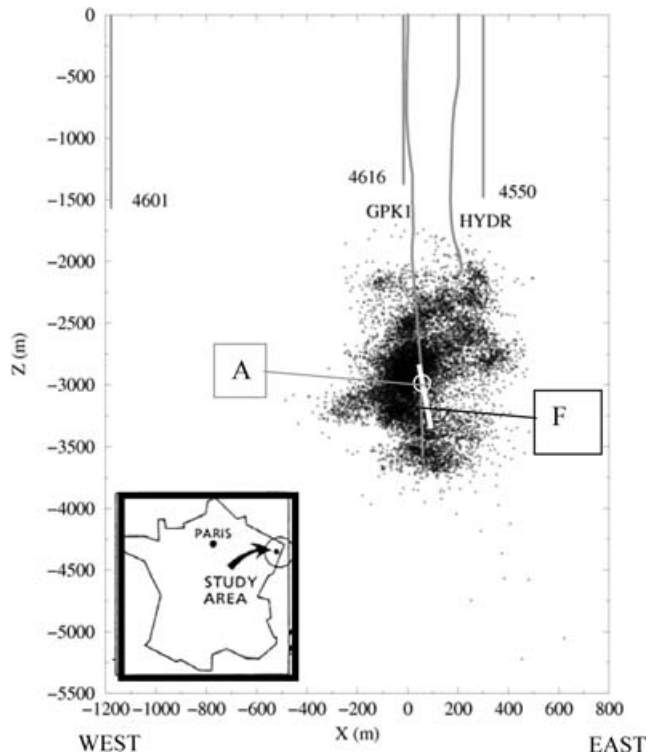

Figure 1. Induced microseismicity at Soultz, 1993 experiment. Vertical, EW cross-section of 17 d of seismicity. 4601, 4616, 4550: 3 comp. stations. HYDR: hydrophone. GPK1: main injection borehole. White segment: location of fault *F*. A: intersection point of fault *F* and GPK1.

For the present study, in order to constrain the creeping process on faults during the injection, we concentrated our analysis on the fault (labelled '*F*') presenting one of the largest slip (4.3 cm of normal faulting), and the largest number of multiplets consistent with its location. The location consistency was defined by assuming that the fault dip and strike can be extrapolated from the borehole measurements at its intersection point A (depth $Z = 2925$ m; strike 138°, dip 86°), allowing an uncertainty of 10° in these angles, and recalling the uncertainty of the absolute position of the events, as well as of point A (25 m). The slipping plane of each selected multiplet could be precisely inferred from the accurate relocation of the events, through a classical master-event technique based on time differences calculated by cross-correlation on *P* and on *S* wave. An example of relocated hypocentres is provided in Fig. 2(b) The resulting uncertainty in relative location of events within a given multiplet is of the order of 1 m, or less, thanks to time correlation accuracies smaller than the sampling rate. We could select 30 such multiplets, representing a total of 400 earthquakes, whose projections on plane *F* and on a vertical plane perpendicular to it are plotted in Fig. 3.

For all the multiplets, we carried out a spectral analysis of the seismograms. The attenuation was estimated by the quality factor $Qp = 150$ for the *P* wave (Bourouis 2004) and $Qs = 127$ for the *S* wave (Gaucher 1998). For the selected events, the corner frequency fc was small enough (range 200–300 Hz) to remain directly visible on the spectra, unaltered by the attenuation which is effective at frequencies larger than 500 Hz, as is illustrated in Fig. 4. For a

© 2007 The Authors, *GJI*, **169,** 723–732
Journal compilation © 2007 RAS

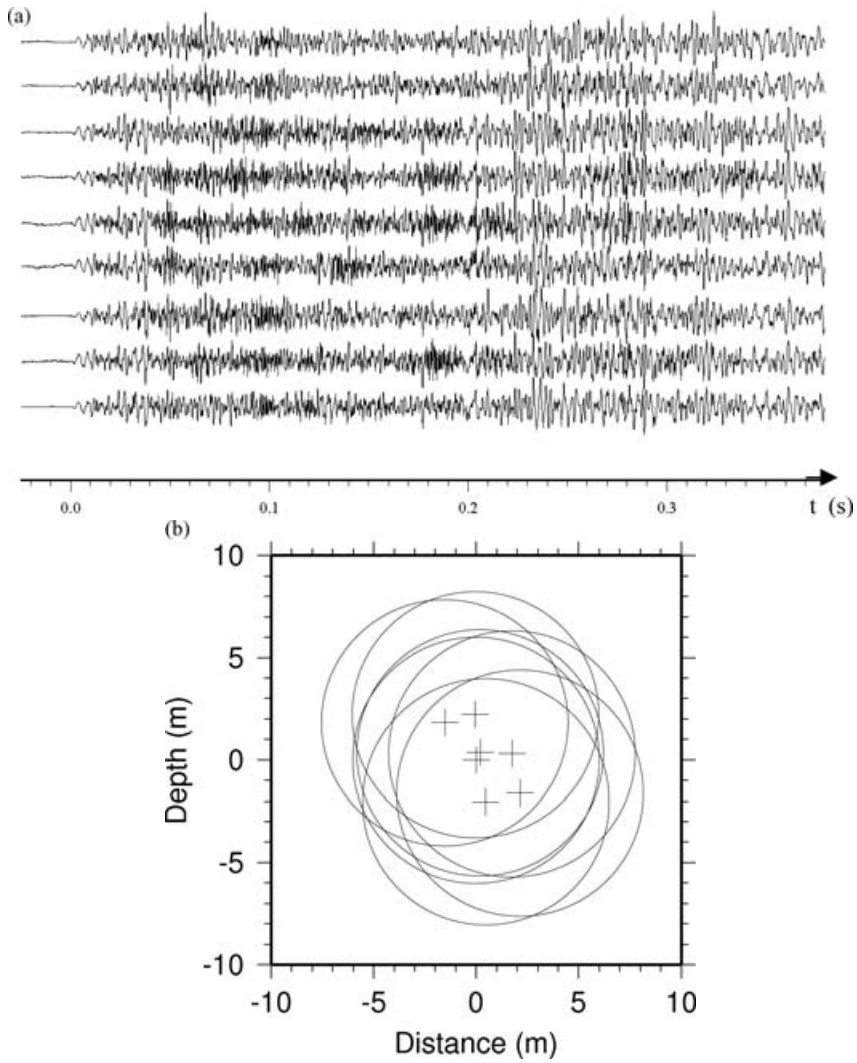

Figure 2. Example of Multiplet. (a): multiplet record; (b): relocated hypocentre of a multiplet and estimated source area (deduced from its corner frequency).

given multiplet, the corner frequency remains stable, although the spectral level (or seismic moment) could vary by a factor up to 20. For each multiplet, one could infer a source radius R of the order of 5 m, using the corner frequency estimate by Brune (1970), $f_c \approx 0.8\ V_s/R$, with an S velocity V_s of 3.34 km s^{-1}. This radius is most of the time larger than the distance between the source barycentres (see Fig. 2b), as determined by cross-correlating P and S waves, which indicates that each multiplet mostly consists of the repeated rupture of the same asperity, with a varying stress drop. Thus, our selected multiplet sequence can be seen as the repeated seismic ruptures of 30 different asperities, distributed all over the whole fault plane F.

4 CUMULATIVE COSEISMIC SLIP AND RUPTURE HISTORY ON FAULT *F*

For each event from a given multiplet/asperity, we estimated the mean coseismic slip, from the source radius and the seismic moment from the seismogram. This slip and the related stress drop is highly variable (from 2 to 40 MPa, under the assumption of Brune's (1971) source size estimate), but does not reveal any trend with time. The time dependent cumulative slip on each asperity is plotted in Fig. 5. It shows that most asperities start their activity in the early stage of the water injection, and that their rupture rate progressively diminishes: the mean slip rate slows down (generic functions in Fig. 5, top). Most of the asperities slip by a few centimetres, and three of them cumulate between 10 and 20 cm. The mean value is about 4 cm. The large variability of final slip may result from both the unaccounted variability of rupture velocities and directivity (leading to erroneous values of radius and stress drop, possibly by a factor up to 2 and 4, respectively), and real variability of slip at different locations on fault F. Despite these uncertainties, and the related possibility that a small proportion of the seismic sources in a given multiplet may not actually overlap the main asperity, the first robust result is that the cumulative slip reaches a few centimetres for most asperities, which is compatible with the slip measured at point A.

The starting time of the rupture of each asperity shows a clear dependence with depth, thus to its distance to point A. The space–time envelope of these events is expected to image the diffusion of the pore pressure head within fault F (dotted line in Fig. 5, bottom left). The first asperity to break (red stars in Fig. 5) accelerates its slip, as a response to an increase of water pressure. The following multiplets can be grouped into different fault segments within which asperities are starting to slip at nearly the same time (within less than a few hours) (segments S_i in Fig. 5). The 0.6 MPa pressure step of day 3 triggers the rupture of the first group of asperities (S_1), but the start of the other groups (S_2, S_3, S_4, ...) does not coincide with

© 2007 The Authors, *GJI*, **169,** 723–732
Journal compilation © 2007 RAS

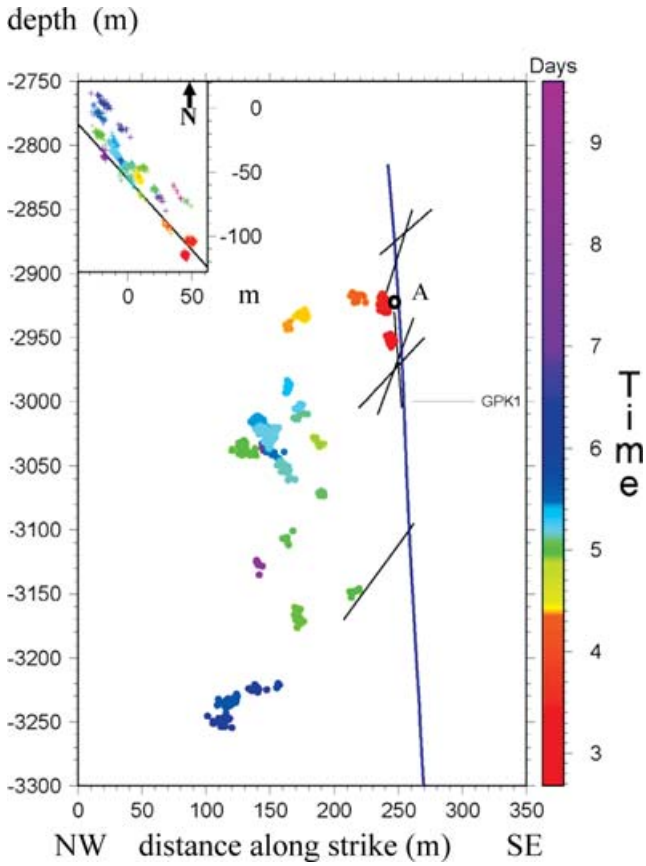

Figure 3. Multiplet/asperity distribution on creeping fault *F*. Rupture time of the asperity is colour-coded. Point A (black circle) is the intersection between *F* and borehole GPK1. Blue line is horizontal projection of the GPK1 borehole. Black segments are activated faults reported from GPK1 logging. Top-left insert: map view of the asperity distribution.

later steps in pressure and flow rate. However, the latter pressure steps induce jumps in the seismicity and in the slip rates of already activated asperities (days 6.5 and 8.5). The largest segment to slip as a whole (S_3) is about 200 m long. The simplest interpretation of this rupture sequence is the progressive pore pressure increase and diffusion within the contiguous fault segments until their strength limit is successively reached.

5 CROSS-TRIGGERING BETWEEN BREAKING ASPERITIES

Some asperities are located very close to each other (see Fig. 3, in particular, between 3010 and 3060 m in depth), leading us to analyse the interevent time distribution for possible cross-triggering of their seismic ruptures. The distribution of distance versus interevent time – or delay – for these neighbouring asperities is presented in Fig. 6 (top), which shows that small delays (less than a few hundreds seconds) are mostly produced by close event pairs (<30 m). This is better quantified in Fig. 6 (bottom), where these two groups are separated: for distances larger than 30 m (triangles), the distribution of the delay density shows a random fluctuation of about 1.5 per 100 s, with no trend in time, consistent with independent ruptures and a Poisson distribution. However, for distances smaller than 30 m (squares), which concerns five distinct multiplet/asperities, the distribution of the binned delays clearly decays with time, with 14 events in the first 100 s, an average of 6 per 100 s in the next 500 s, then reaching a background noise level of 0–1 per 100 s in the next

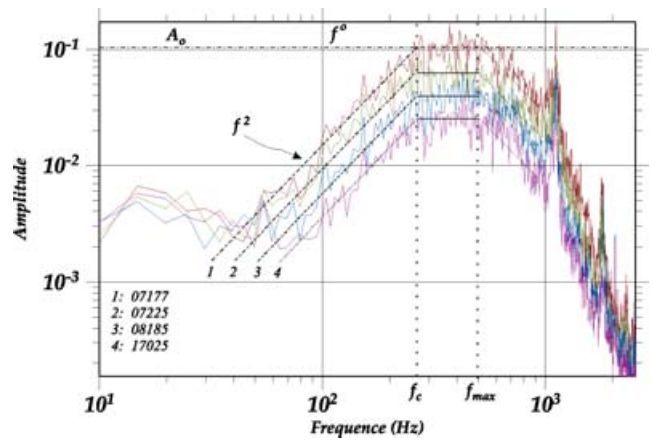

Figure 4. Example of *P*-wave acceleration spectra of a single multiplet. Each spectrum is an average of the two stations 4550 and 4616. Note the constancy of the corner frequency, despite the variation in spectral amplitude for the four selected events.

thousands seconds. This provides evidence for clear interaction between neighbouring asperities, with a significantly larger rate for times smaller than a few hundreds of seconds.

For the interacting asperities (distance <30 m), the delays are all larger than 10 s, much larger than the individual rupture durations. Thus, each dynamic rupture slows down and stops 10–100 s before triggering the neighbouring asperity. This suggests that the interacting asperities are not contiguous, that is, that their weakening areas are significantly apart, separated by relatively large areas with strengthening properties or high surface energy. This is consistent with the 5 m source radius estimated above. It may also be consistent with the largest sources, of about 10 m in radius. Indeed, as one expects that the dynamic rupture decelerates within the strengthening part of the fault around the weakening asperity, the seismic estimate of the source size may overestimate the size of the latter. Consequently, for contiguous seismic sources with a 10 m radius (i.e. with 20 m of separation between their centroids), one expects that the slip area of the first asperity to break remains significantly distant from the weakening part of the second asperity, preventing immediate dynamic triggering.

6 INTERPRETATION: SEISMIC VERSUS ASEISMIC SLIP ON FAULT *F*

The global picture for fault *F* is that its large-scale creep history is mapped by the cumulative slip of its asperities. A similar approach was already used for analysing multiplets on the steadily creeping sections of the San Andreas fault (Nadeau & McEvilly 1999). However, at Soultz, the average slip presents an early fast rate which decays with time roughly as $l/(1 + t/\tau)$ (time constant τ of the order of a few hours). This behaviour is typical of triggered creep and afterslip reported for shallow faults (e.g. Marone *et al.* 1991), involving rate-strengthening friction laws. We thus interpret the slip history of *F* as resulting from the rapid decrease of the effective normal stress (through the pore pressure increase related to the injection) on a globally rate-strengthening surface. This 'large-scale' slow slip forces the repeated seismic ruptures of small asperities scattered on *F*, which all obey a weakening friction law.

Fault *F* can be divided into a few segments (Si), each involving a group of asperities initiating their rupture at nearly the same time. Each segments has its own slow slip history, triggering with some

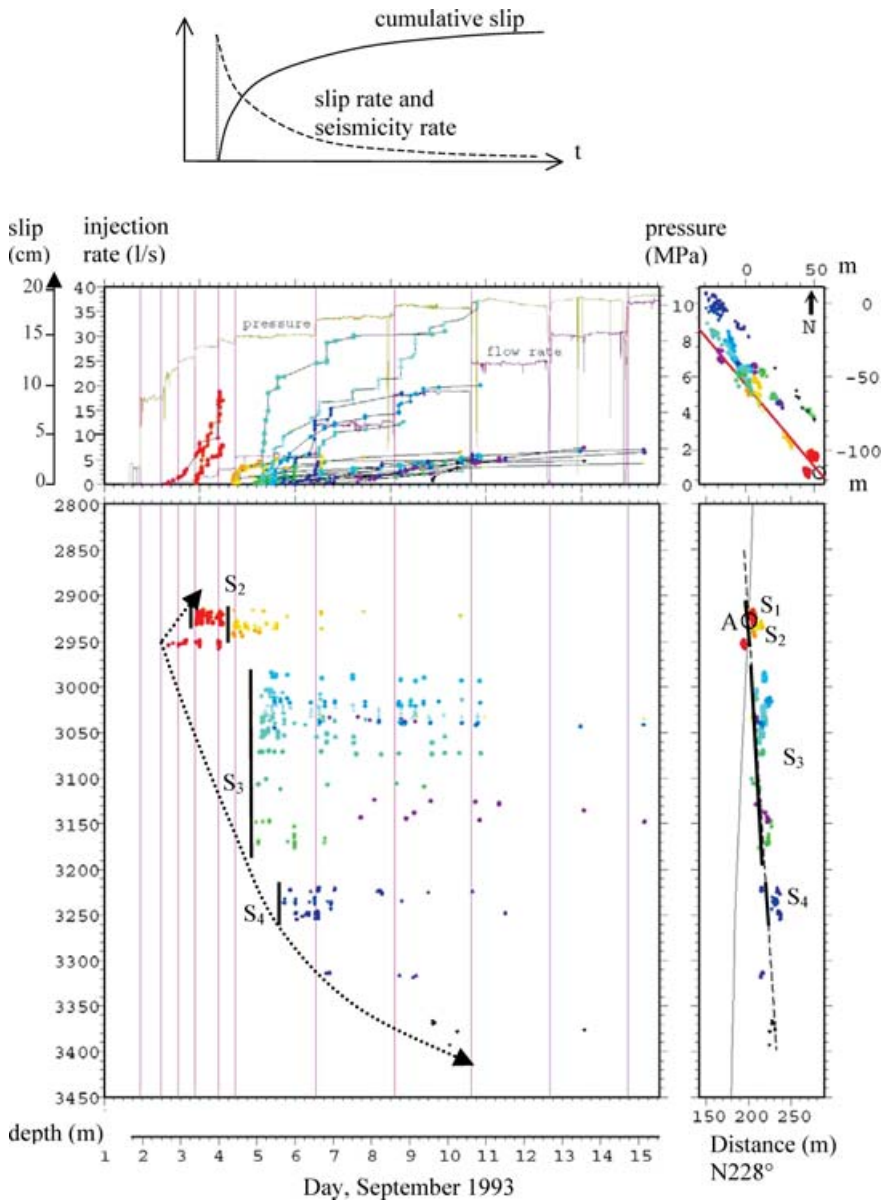

Figure 5. Asperity rupture history on fault *F*. top: generic processes versus time; middle left: borehole water pressure, injection flow rate and cumulative slip for each multiplet; bottom left: depth of events, versus time; middle right: top view of the multplets and fault *F*; bottom right: vertical cross-section of multiplets. Multiplets are colour coded. Si indicate the inferred fault segments.

delay the rupture of the next deeper one, and so on. This cascade of slow events is expected to be the consequence of fluid pressure migration within the fault zone, combined with a mechanical interaction (static Coulomb type) between slipping segments. However, the rupture of each segment as a whole suggests the dominance of a rather homogeneous pore pressure effect, at least for S_3. Indeed, a solid-elastic interaction would have shown delayed, progressive activation of asperities along the segment, due to the short range, stress concentration at fracture tips—which is not observed.

The delay in creep initiation time between the different segments suggests that fault *F*, as a whole (about 400 m long), may be considered as a new fault, in the sense that it may be the first time that these segments have been connected through fresh fractures, and forced to slip during the same slow event. The pre-injection loggings showed the pre-existence of fracture *F* at point A, but the latter was similar to the many other fractures revealed by the logging. Thus, this fracture was not particularly developed before injection. The other, larger fault segments which we identified on *F* were also probably pre-existing, being themselves possibly segmented at a smaller scale, and reactivated in creep during the injection. This evidence for the formation of a new fault, by connecting smaller fault segments, has important implications in the mechanical processes at work in the Soultz hydrofracturation experiment, and in the permeability modification of the granite body (Jones *et al.* 1995).

The log $(1 + t/\tau)$ mean slip history corresponds to a seismicity rate of $1/(1 + t/\tau)$ for the multiplets. This fits the standard Omori law, decaying as $1/tp$ for large times, with $p = 1$. The stack of the multiplet sequences, presented in Fig. 7(a), allows to better constrain the exponent p in the range 0.80–0.85. Without our detailed study on the slow slip, these events could have been interpreted as 'aftershocks' directly triggered by the water injection. Under the standard interpretation of the Dietrich friction law (Dieterich 1994; Dieterich

© 2007 The Authors, *GJI*, **169,** 723–732
Journal compilation © 2007 RAS

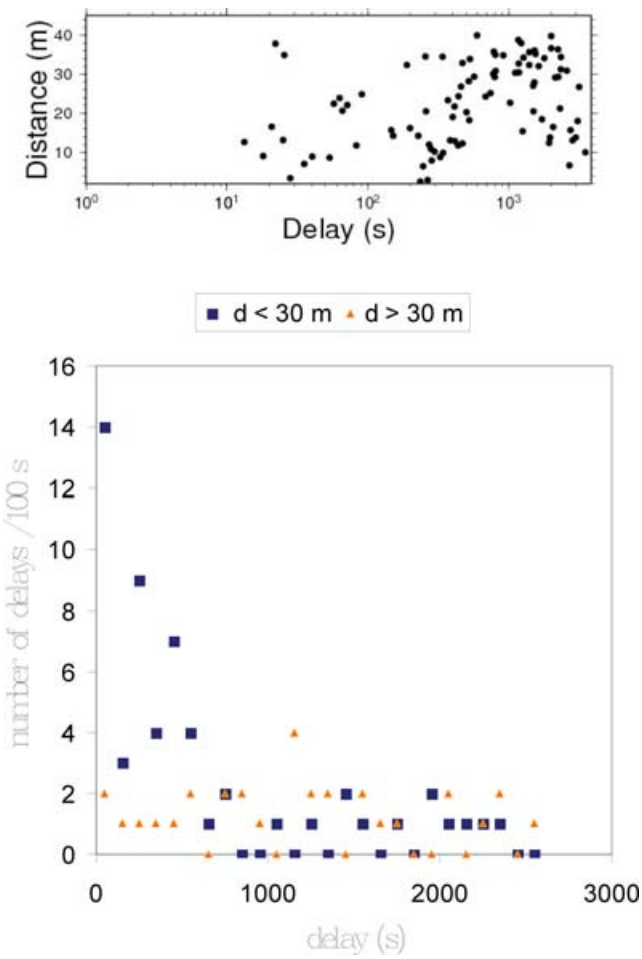

Figure 6. Rupture cross-triggering between neighbouring asperities: Top: distance between asperities versus interevent time delay. Bottom: statistics of interevent times for $d > 30$ m (triangles) and $d < 30$ m (squares).

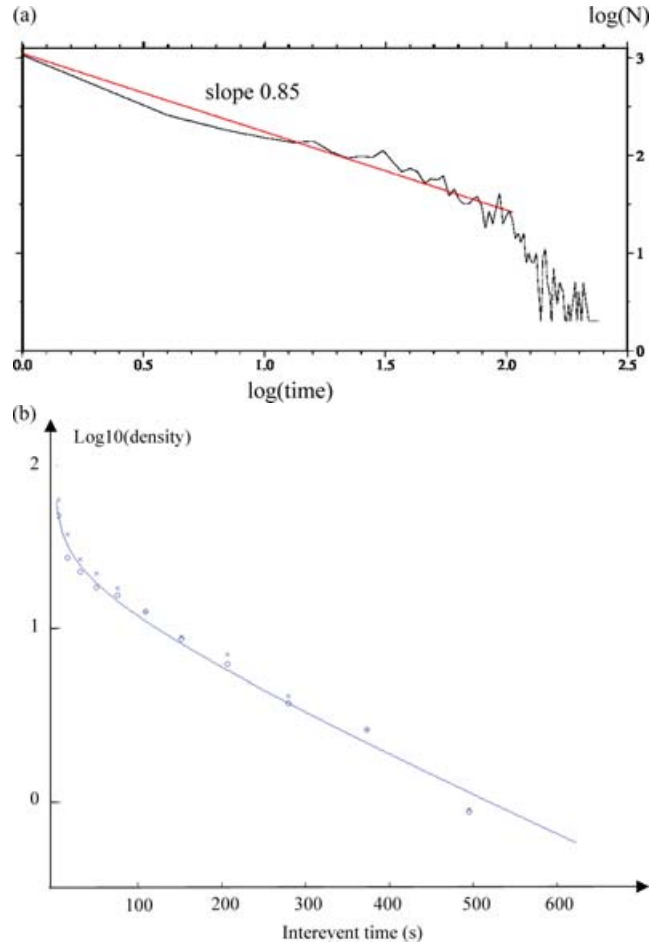

Figure 7. (a) Distribution of event times in multiplets. For each multiplet, the first event is assigned time zero. Timescale in hours. The global distribution is obtained by stacking the distributions of all multiplets. This can be seen a composite Omori law with respect to the start of the multiplet. (b) Interevent time distributions. Circles: density (number per second) of delay times for the singlet population; crosses: density of delay times for the multiplet population (doublets and larger multiplets). Black curve: Gamma distribution with $\gamma = 0.7$ and $\beta = 1.7$, scaled in time by the mean delay $t_o = 125$ s (see text).

et al. 2000), the Omori law would then have been erroneously interpreted as resulting from the weakening frictional property of the asperities. Our results show to the contrary that the origin of this decay in seismicity rate is due to the strengthening law of the creeping areas of the fault, around the asperities, consistent with the interpretation of aftershock sequences by Perfettini & Avouac (2004), as will be discussed later.

A standard rate-strengthening friction law (e.g. Marone *et al.* 1991) is well suited for the rupture of segments S_1 and S_4, as the creep velocity jump coincides with the pore pressure step. For S_2 and S_3, there is no evidence for coincident pressure change at the borehole head: the simplest explanation, compatible with such a friction law, would be the occurrence of a fast (<1000 s) local pore pressure increase and diffusion within the fault segment, coupled with a sudden permeability increase due to its opening. The latter would be delayed with respect to the forcing pressure at the borehole by initially low permeability. The absence of delay for segments S_1 and S_4 can be explained for S_1 by the proximity to the borehole, and for S_4 by the probably high permeability increase of S_3, favouring fast pore pressure diffusion.

The interpretation above rely on the assumption that the selected multiplets belong to the same fault surface F. If this assumption is relaxed, one has to introduce a set of parallel, creeping faults, each of which would reach a final slip of the order of a few centimetres, as deduced from the multiplets they would activate. Simple stress drop scaling laws then lead us to assign to each of these faults a minimal length of several tens to a few hundreds of metres. The resulting global strain would thus be many times larger than that produced in our model by fault F alone, which is not realistic, as the latter is already very large (typically 1 cm/100 m, that is, 10^{-4}). Our hypothesis of a single fault embedding the selected multiplets is thus not only simpler, but also much more realistic.

Considering the dominance of multiplets over singlets in the 1993 microseismicity at Soultz, together with the other reported fracture activation within the borehole, we suggest, after Cornet *et al.* (1997), that a dominant part, if not most, of the global strain induced by the water injection in the reservoir occurred by aseismic slip on faults, such as F, with dimensions ranging from several tens of metres to several hundreds of metres – and by the formation (or growth) of new, large faults. The centimetric shear displacement on these faults are expected to be the dominant cause of the large permeability enhancement reported by Evans *et al.* (2005).

The way this large strain transient triggered the recorded singlet-type seismicity is not resolved: these singlets could be either related

to asperities which are forced to rupture only once by creep around them, following the same model as for our selected multiplets, or to isolated fractures which respond to the slow strain evolution in the rock volume, following Dietrich's (2000) model. A way to compare the singlet and the multiplet populations is to analyse their clustering characteristics as evidenced by the distribution of their interevent times (e.g. Hainzl *et al.* 2006). The density of interevent times (number per second) is plotted in Fig. 7(b) for the singlets (circles) and the multiplets (crosses), together with a Gamma distribution of the form $(t/t_o)^{(\gamma-1)}e^{-t/\mathrm{to}*1/\beta}$. The values $\gamma = 0.7$ and $\beta = 1.7$, with a recorded mean interevent time $t_o = 125$ s ($t_o = 129$ s for the singlets and $t_o = 121$ s for the singlets), provides a reasonable fit to both data sets. The decay for large interevent times describes the poissonian part of the process, and the value of $1/\beta = 0.6$ provides the proportion of independent events. The behaviour for small interevent times ($t < t_o$), characterized by $\gamma = 0.7$, shows clustering ($\gamma = 1$ would correspond to a stationary Poisson process, $\gamma = 0$ to a single Omori-type sequence with exponent 1). The observed match between singlet and multiplet behaviour for the clustering at small delays suggests the existence of a common cross-triggering mechanism.

In conclusion for the Soultz 1993 induced seismicity, the strain source for the singlet and multiplet seismic activity is thus expected to mostly result from the creeping of a few faults, the latter being triggered by pore-pressure increase and probably modulated by the fault interactions.

7 IMPLICATIONS FOR SEISMOGENIC TRANSIENTS

7.1 Implications for the origin of the Omori law in aftershock sequences

In seismic regions, the possibility that some Omori-type sequences of repeating aftershocks may be due to strengthening friction on major creeping faults was first documented in Schaff *et al.* (1998). These authors analysed some multiplets following the 1989 Loma Prieta earthquake, and interpreted their rate with the slowing down of afterslip on the main fault surface. Our study thus confirms, with more detailed evidence, the existence of such processes.

This non-standard explanation of the Omori law was developed further in Perfettini & Avouac (2004), for whole aftershock sequences, by considering brittle creep on the main fault zone. This was illustrated by the correlation between the GPS post-seismic displacement and the aftershock decay rate for the 1999 Chi-Chi earthquake. The assumption was that the seismicity rate is proportional to the sliding velocity of the shear zone. However, no details was provided on the geometrical characteristics of interactions at a local scale between the aseismic and the seismic portions of the fault(s).

The asperity model presented here, conceived for multiplets, can also be considered for non-repetitive ruptures and may thus be appropriate for the aftershock model in Perfettini & Avouac (2004). Indeed, as demonstrated in Appendix A, and Fig. 8, even if the stress perturbation and the resulting creep are too small for breaking any asperity more than once, the statistics of rupture of many asperities should display an Omori type rate. The case of Soultz is consistent with this model, as the interevent time distribution of the selected multiplet/asperities is similar to that of the recorded singlets. Such an asperity model thus provides a small scale, detailed picture of what may actually be happening during the post-seismic phase not only

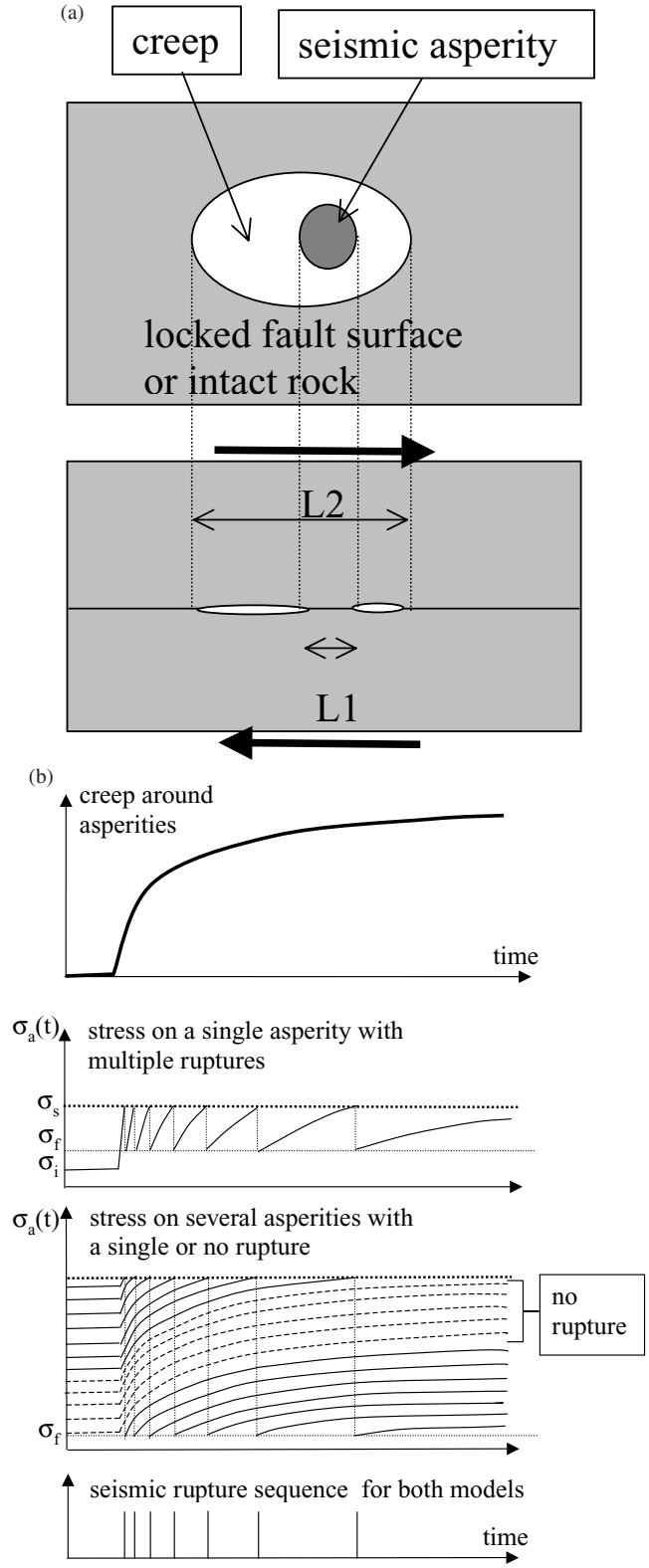

Figure 8. (a) Asperity model. Top: view of the fault plane; bottom: section across the fault plane. (b) Omori law triggered by post-seismic or relaxation creep around asperities. From top to bottom: model of creep deceleration forcing the rupture of asperities such as in (a); resulting stress on a single asperity resulting on multiples ruptures; resulting stress on asperities triggering a single or no rupture; resulting seismic sequences, equivalent for the two models above.

© 2007 The Authors, *GJI*, **169,** 723–732
Journal compilation © 2007 RAS

within the main creeping fault zone where afterslip dominates, but also on the many isolated, smaller faults within the whole perturbed crustal volume.

7.2 Implications for multiplet diagnostic in seismogenic regions

Our results provide direct evidence that multiplets in a seismic sequence can be diagnostic of the existence of seismic asperities embedded on a slowly slipping fault surface. It thus extends for small scale creeping faults (tens to hundreds of metres) the few similar observations concerning the large creeping section of major faults. During a seismic swarm with multiplets, the evaluation of the size and dynamics of the latter may reveal the size of the slipping patches and their cumulative slips, thus allowing to estimate the resulting hydromechanical perturbations in their surroundings.

As natural hydrostimulation involves high pore pressure and reduced effective stresses, it should enhance fault creep and hence repeated ruptures of asperities, like in Soultz. The existence of multiplets sequences within a seismic swarm might thus indicate such processes. Furthermore, the space–time evolution of these multiplets might better reveal the water pressure paths than the evolution of the usually dominant, singlet-type microseismicity of the swarm: indeed, they are diagnostic of large aseismic slip, thus likely to be associated with large increase of permeability. A major difficulty, however, is that multiplets may not be easily detected from standard surface seismic arrays: in particular, none of the 1993 multiplet sequences of Soultz were detected with the surface seismic array, which stresses the importance of high-resolution borehole seismic arrays.

7.3 Implications for friction laws and transients on seismogenic faults

The frictional behaviour of creeping faults with asperities, similar to fault *F* at Soultz, results from the combined effect of the creeping area (strengthening) and of the seismic asperities (weakening). The effective friction coefficient can be approximated by an average of the 'creep' and 'seismic' coefficients, weighted by their respective contact area. The creep component can be largely dominant, like at Soultz, but increasing the proportion of asperities should eventually lead to a globally weakening friction – and thus to possible large earthquakes resulting from the activation of all neighbouring asperities in the same dynamic rupture.

Considering that for any fault surface, one may define an average asperity density, a 'critical' asperity density might be defined, above which a fault surface becomes unstable and entirely seismic. Note that the critical density is not reached on fault *F* at Soultz: even the closest asperity pairs (distance <30 m) did not succeed to trigger each other in a larger dynamic rupture, as evidenced by their delay in cross-triggering (tens of seconds).

We believe that faults areas exhibiting near-critical densities of asperities are expected to produce non-standard frictional behaviour, prohibiting simple up-scaling and averaging of friction laws defined at the smallest scale, and to favour the development of transient creep at various scales in time and space. This would be, in particular, consistent with the picture of transients, precursors, and main shock hypocentres, being located near the deep transition zone between stable and unstable areas of major faults (Fig. 9).

For instance, within the mostly creeping sections of the San Andreas and the Calaveras faults, the space–time pattern of

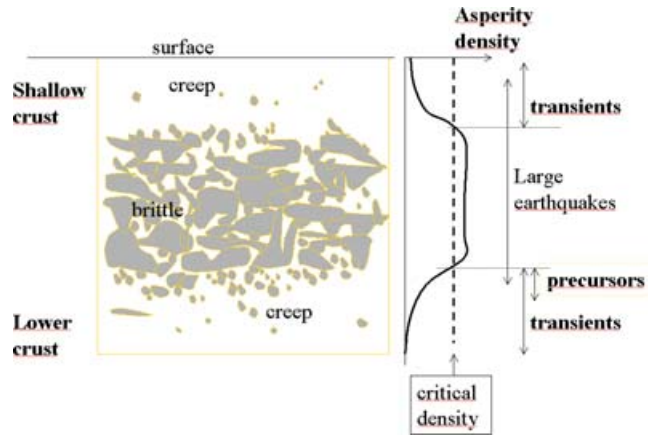

Figure 9. Sketch of speculative asperity density distribution in the crust.

microearthquake interaction presented by Rubin (2002) reveals that neighbouring asperities do not rupture dynamically in large cascade events, despite their distances at less than one source dimension, thus implying a subcritical density of asperity contacts. Some of the recently observed tectonic tremors in the Cascades (Rogers & Dragert 2003), in Japan (Obara 2002) and in California (Nadeau & Dolenc 2005), might also represent a 'subcritical' creeping process – possibly involving fluid migration, as in Soultz – with an asperity density possibly close to critical.

The possibility that transients processes (including aftershock sequences and large rupture initiation) strongly depend on the strengthening properties of creeping faults and less on the friction properties of weakening asperity contacts, has important consequences for the dependence of these friction models on pore pressure. Indeed, both type of fault zones are expected to have very different sensitivities to pore pressure (resulting from very different hydraulic conductivities and/or storage capabilities), differences which should lead to different creep or fluid transient characteristics.

8 CONCLUSION

We have shown that at Soultz, most of the induced seismicity during the 1993 hydraulic stimulation experiment was forced by large-scale strain induced by centimetric creep on hectometric fault segments. This lead to a largely dominant aseismic strain within the hydrofractured volume, and to the formation of new, large faults. The studied Soultz multiplets mostly appear as repeaters (i.e. the repeated rupture of single asperities), allowing the study of their cumulative slip, forced by the aseimic creep around them, and revealing the strengthening properties of the creeping part of the faults.

Our model significantly differs from the standard explanation for induced seismicity during water injection experiments: in the latter, seismicity is assumed to be due to Coulomb stress failure directly caused by pore pressure increase within the weakening area – that is, within the seismic fracture. In Soultz, the multiplet seismicity is shown to be dominantly due to shear stress concentration on asperities, generated by creep within the surrounding, aseismic part of the fault, this creep being the consequence of pore pressure increase within this strengthening portions of the fault zone. Thus, in Soultz, the role of permeability and pore pressure increase within the weakening part of the fractures is found to be marginal, in a first approximation.

More generally, these results support the idea that observations of multiplets in seismogenic regions can be diagnostic of fault creep,

possibly triggered by fluid flow. Our interpretation of the microseismicity rate of the asperity ruptures in terms of the strengthening properties of the surrounding creeping fault can be generalized for non repeating ruptures, and in particular, for aftershock sequences, suggesting that a significant part of the Omori law decay rate might be controlled by creeping faults at al scales. This makes, in particular, the link between the general fault model proposed by Perfettini & Avouac (2004) and the specific observation by Schaff *et al.* (1998).

The observations of space–time distributions of asperities at Soultz also lead us to introduce the simple concept of asperity densities (relative value of weakening friction area over total area) on fault planes. It implies the existence of critical density value, above which dynamic rupture sweeping across many asperities is favoured, around which seismic transients and precursors are expected, and below which aseismic creep (with possible transients) is dominant.

Finally, our results imply that analysing aftershocks or regional seismicity with models involving only static or dynamic interaction between seismic faults at different scales, like in epidemic models, may be very misleading, as a significant part of the stress change at the origin of the microseismic activity might result from triggered aseismic slip on fractures and faults. Direct, high resolution strain measurements (with borehole strainmeters or long base tiltmeters) are thus requested to correctly identify and model the sources of strain within the fault systems at depth, coupling microseismicity, creep and fluid flow instabilities. Following Bernard (2001), such studies are, in particular, requested for progressing on the question of earthquake precursors, which can be considered as the specific subclass of those transients which managed to grow up and degenerate into a large, dynamic rupture.

ACKNOWLEDGMENTS

We are very grateful to R. Jones and the Camborne School of Mines Associates for providing us the 1993 Soultz seismological records. We thank H. Perfettini and an anonymous reviewer for their constructive comments, which helped to clarify and improve the paper. This work also benefited from discussions with *F*. Cornet on the triggered seismicity and stress conditions at Soultz.

REFERENCES

Bernard, P., 2001. From the search of 'precursors' to the research on 'crustal transients', *Tectonophysics,* **338,** 225–232.

Bosl, W.J. & Nur, A., 2002. Aftershocks and pore fluid fiffusion, following the 1992 Landers earthquake, *J. geophys. Res.,* **107** (B12), 2366, doi:10.1029/2001JB000155.

Bourouis, S., 2004. Sismicité induite et comportement mécanique d'un massif granitique fracturé par injection d'eau. Application au site géothermique de Soultz-sous-Forêts, *PhD thesis*, IPGP/University of Paris 7 (in French).

Brune, J., 1970. Tectonic stress and the spectra of seismic shear waves from earthquakes, *J. geophys. Res.,* **75,** 4997–5009.

Bürgmann, R., Ergintav, S., Segall, P., Hearn, E.H., McClusky, S., Reilinger, R.E., Woith, H. & Zschau, J., 2002. Time-space variable afterslip on and deep below the Izmit earthquake rupture, *Bull. seism. Soc. Am.,* **92,** 138–160.

Cornet, F.H., 2000. Comment on 'Large-scale in situ permeability tensor of rocks from induced microseismicity by S. A. Shapiro, P. Audigane and J.-J. Royer, *Geophys. J. Int.,* **140,** 465–469.

Cornet, F.H., Helm, J., Poitrenaud, H. & Etchecopar, A., 1997. Seismic and Aseismic Slips Induced by Large Scale Fluid Injections; *Pure App. Geophys.,* **150,** 563–583.

Dieterich, J.H., 1978. Time Dependent Friction and the Mechanisms of Stick-Slip, *Pure Applied Geophysics,* **116,** 790–806n.

Dieterich, J., 1994. A constitutive law for rate of earthquake production and its application to earthquake clustering, *J. geophys. Res.,* **99,** 2601–2618.

Dieterich, J., Cayol, V. & Okubo, P., 2000. The use of earthquake rate changes as a stress meter at Kilauea volcano, *Nature,* **408,** 457–460.

Dragert, H., Wang, K. & James, T.S., 2001. A silent slip event on the deeper Cascadia subduction interface, *Science,* **292,** 1525–1528.

Elsass, P., Aquilina, L., Beauce, K., Benderitter, Y., Fabriol, H., Genter, A. & Pauwels, H., 1995. Deep structure of the Soultz-sous-Forêts HDR site (Alsace, France), in proc. World Geotherm. Cong., Florence, Italy, pp. 2543–2647.

Evans, K.F., Moriya, H., Niitsima, H., Jones, R.H., Phillips, W.S., Genter, A., Sausse, J., Jung, R. *et al.*, 2005. Microseismicity and permeability enhancement of hydrogeologic structures during massive fluid injections into granite at 3 km depth at the Soultz HDR site, *Geophys. J. Int.,* **160,** 388–412.

Gaucher, E., 1998. Comportement hydromécanique d'un massif fracturé: apport de la microsismicité induite. Application au site géothermique de Soultz-sous-Forêts, *PhD thesis*, Univ. Paris 7 (in French), 245 pp.

Gladwin, M.T., Gwyther, R.L., Hart, R.H.G. & Breckenridge, K.S., 1994. Measurements of the strain field associated with episodic creep events on the San Andreas fault at San Juan Bautista, California, *J. geophys. Res.,* **99,** 4559–4565.

Gomberg, J., Reasenberg, P.A., Bodin, P. & Harris, R.A., 2001. Earthquake triggering by seismic waves following the Landers and Hector Mine earthquakes, *Nature,* **411,** 462–466.

Gwyther, R.L., Gladwin, M.T., Mee, M. & Hart, R.H.G., 1996. Anomalous shear strain at Parkfield during 1993–1994, *Geophys. Res. Lett.,* **23,** 2425–2428.

Hainzl, S. & Fisher, T., 2002. Indications for a successively triggered rupture growth underlying the 2000 earthquake swarm in Vogtland/NW-Bohemia, *J. geophys. Res,,* **107**(B12), 2338, doi:10.1029/2002JB001865.

Hainzl, S., Scherbaum, F. & Beauval, C., 2006. Estimating background activity based on interevent-time distribution, *Bull. seism. Soc. Am.,* **96,** 313–320.

Heim, J.A., 1996. Aléa sismique naturel et sismicité induite du projet géothermique européen RCS (Roche Chaude Sèche) De Soltz-sous-Forêts (Bas-Rhin, France). PhD Thesis, Université Louis Pasteur/EOPGS, Strasbourg.

Helmstetter, A. & Sornette, D., 2003. Importance of direct and indirect triggered seismicity in the ETAS model of seismicity, *Geophys. Res. Lett.,* **30,** 11, 1576–1579.

Hickman, S., Sibson, R. & Bruhn, R., 1995. Introduction to special session: mechanical involvment of fluids in faulting, *J. geophys. Res.,* **100,** 12 831–12 840.

Jones, R.H., Beauce, A., Jupe, A., Fabriol, H. & Dyer, C., 1995. Imaging induced seismicity during the 1993 injection test at Soultz-sous-Forets; in *World Geothermal Congress,* Florence, Italy, Vol. 4, pp. 2665–2669, International Geothermal Association, San Diego.

Linde, A.T., Gladwin, M.T., Johnston, M.J.S., Gwyther, R.L. & Bilham, R.G., 1996. A slow earthquake sequence on the San Andreas fault, *Nature,* **383,** 65–68.

Lowry, A., Larson, K., Kostoglodov, V., Bilham, R., 2001, Transient fault slip in Guerrero, southern Mexico, *Geophys. Res. Lett.,* **28,** 3753–3756.

Marone, C.J., Scholz, C.H. & Bilham, R., 1991. On the Mechanics of earthquake afterslip, *J. geophys. Res.,* **96,** 8441–8452.

Obara, K., 2002. Non-volcanic deep tremor associated with subduction in Southwest Japan, *Science,* **296,** 1679–1681.

Miller, M., Melbourne, T., Johnson, D.J. & Sumner, W.Q., 2002. Periodic slow earthquakes from the Cascadia subduction zone, *Science,* **295,** 2423.

Nadeau, R. & McEvilly, T.V., 1999. Fault slip rates at depth from recurrence intervals of repeating microearthquakes, *Science,* **285,** 718–721.

Nadeau, R.M. & Dolenc, D., 2005. Tremor activity before and after the 2004 Parkfield earthquake, *Seism. Res. Lett.,* **76,** 216.

Obara, K., 2002. Nonvolcanic deep tremor associated with subduction in southwest Japan, *Science,* **296,** 1679–1681.

Perfettini, H. & Avouac, J.P., 2004. Post-seismic relaxation driven by brittle creep: A possible mechanism to reconcile geodetic measurements and the decay rate of aftershocks, application to the Chi-Chi earthquake, Taiwan, *J. geophys. Res.,* **109**(B2), 2304, doi:10.1029/2003JB002488.

Rubin, A.M., 2002. Aftershocks of microearthquakes as probes of the mechanics of rupture, *J. geophys. Res.,* **107,** 101029/2001JB000496.

Rogers, G. & Dragert, H., 2003. Episodic tremor and slip on the Cascadia Subduction: The chatter of Silent slip, *Science,* **300,** 1942–1943.

Schaff, D.P., Beroza, G.C. & Shaw, B.E., 1998. postseismic response of repeating aftershocks, *Geophys. Res. Lett.,* **25,** 4549–4552.

Scholz, C., 1998. Earthquake and friction laws, *Nature,* **391,** 37–41.

Shapiro, S.A., Audigane, P. & Royer, J.-J., 1999. Large-scale in situ permeability tensor frocks from induced microseismicity, *Geophys. J. Int.,* **137,** 207–213.

Shibazaki, B. & Iio, Y., 2003. On the physical mechanism of silent slip events along the deeper part of the seismogenic zone, *Geophys. Res. Lett.,* **30**(9), 1489, doi:10.1029/20036L017047.

Sibson, R.H., 1992. Implications of fault-valve behaviour for rupture nucleation and recurrence, *Tectonophysics,* **211,** 283–293.

Stein, R.S., 1999. The role of stress transfer in earthquake occurrence, *Nature,* **402,** 605–609.

APPENDIX A

Consider, on a fault surface, a single seismic asperity with size L_1, surrounded by an aseismic region of dimension L_2 acting as a stress concentrator and obeying a rate-strengthening friction law (Fig. 8a). A remote, step-like change of stress, $\Delta\sigma$, is applied on the volume around this surface (or a pore pressure step within the fault zone), leading the aseismic surface to slip at a $1/t$ rate. We note σ_i the initial stress on the asperity, σ_f its final value after one rupture, σ_s the strength of the asperity. If $\Delta\sigma \times L_2/L_1$ is large enough, then the aseismic slip around the asperity and the resulting stress on the latter, σ_a, will succeed into triggering several seismic ruptures, at a rythm following the $1/t$ slip rate, just as for the multiplets at Soultz. If not, then the asperity may not rupture, or only once, depending on the initial level σ_i. In that case, considering a uniform distribution of σ_i, the probability of rupture of the asperity during the decelerating creep will still be proportional to $1/t$, as shown in Fig. 8(b). Thus, considering a large number of asperities in a seismogenic volume, one expects a statistical rate of events following the $1/t$ Omori law. This remains valid if the aseismic area does not completely encircle the asperity, or if it contains several asperities.

© 2007 The Authors, *GJI*, **169,** 723–732
Journal compilation © 2007 RAS